Wind-Wave Interactions under Hurricane Conditions: A Decade of Progress

James Doyle[1], Peter Black[2], Clark Amerault[1], Sue Chen[1], Shouping Wang[1]

[1] Naval Research Laboratory, Monterey, CA, USA
[2] SAIC, Monterey, CA, USA

Abstract

In the past decade, there have been significant advancements in our understanding and ability to accurately model wind-wave interactions that occur under hurricane conditions. New observations, laboratory measurements, coupled models, and theoretical approaches have all contributed to these new advancements. In this paper, several of these advancements in area of wind-wave interactions that have occurred over the past decade are highlighted.

1. Introduction

The energy source for tropical cyclones (TCs) is primarily attributable to the release of latent heat due to condensation of water vapor (e.g., Ooyama 1969). The exchange of heat, momentum and moisture between the air and sea modulates the distribution of water vapor and heat in the boundary layer and provides the essential link for TCs between the underlying ocean and atmospheric deep convection (and latent heat release). Thus, the exchange of heat, momentum and moisture at the air-sea interface has profound implications for tropical cyclones. In the past decade, a great deal of attention has been focused on gaining a better understanding of the interactions between the atmosphere and ocean during TC passage since it is recognized that the ocean can have a large impact on TC intensity. However, the observations at the air-sea interface in high-wind conditions have been insufficient in order to unravel the intricacies of these air-sea interaction processes.

Emanuel (1986) derived a theory for the potential intensity of a TC that is a function of the local environment and is proportional to the ratio of the bulk enthalpy and momentum exchange coefficients, C_K/C_D. Emanuel (1995) used idealized simulations and theoretical considerations to provide further support that TC intensity is intimately connected with the ratio C_K/C_D. This ratio most likely lies in a rather limited range, 1.2-1.5, in the high wind regime for strong storms, with the threshold for tropical cyclone development lying near 0.75. These findings underscore the overall fundamental importance of air-sea interaction for tropical cyclones.

In the past decade, there have been considerable advances through new air-sea interaction observations, models, and theory related to tropical cyclones. Additionally, a number of new advances have been made to representations of air-wave interaction process in models, as well as advancements in coupled interfaces for fully coupled air-wave-ocean models. In this paper, we will highlight some of these observational and modeling advances related to air-wave interactions under hurricane conditions. To accomplish this, we partially draw on the recent excellent summary of the current state-of-the-science of air-sea interaction in tropical cyclones compiled by Shay (2011).

2. Waves beneath hurricanes

The primary energy source for ocean surface waves is intrinsically related to characteristics and evolution of surface winds. In tropical cyclones, the wind distribution can vary greatly, ranging from axisymmetric to highly asymmetric. Additionally, the radius of maximum winds (RMW) can range from small storms with values less than 20 km to well over 100 km.

In the past decade, the stepped-frequency microwave radiometer (SFMR) onboard the NOAA hurricane hunter aircraft (P3) has been a breakthrough instrument that allows for considerably more accurate surface wind observations in the TC core and outer regions of the storm (e.g., Uhlhorn et al. 2007). SFMR observations are now routinely used to contruct wind field distribution for tropical cyclones. As an example, Fig. 1 shows three H*Wind analyses (Powell et al. 2010) of observations that include SFMR measurements for Hurricanes Emily, Katrina, and Wilma. Emily and Wilma exhibit marked asymmetries, in contrast to Katrina, which has a more axisymmetric distribution, although still contains important asymmetries in the outer wind field. The size and structure of the TC wind field obviously have an important impact on the surface wave generation and air-sea interaction characteristics. It should be noted that current generation numerical weather prediction models are relatively poor at predicting TC intensity and structure.

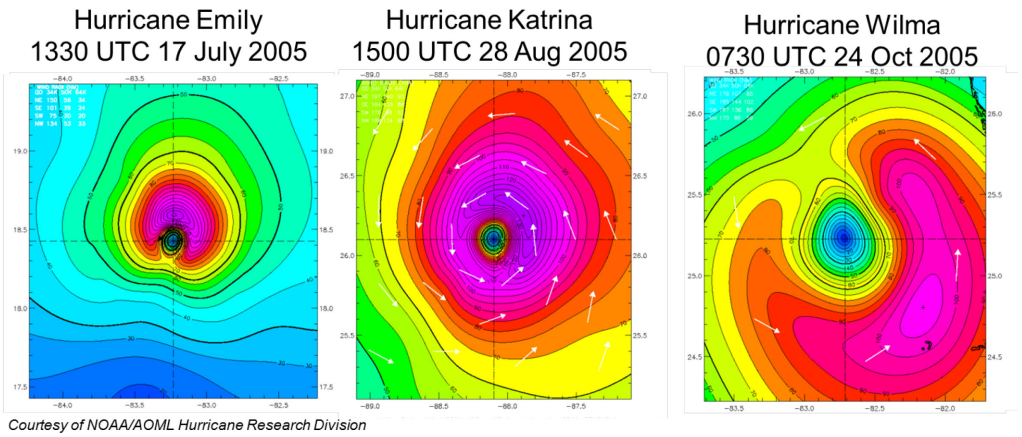

*Figure 1. H*Wind analyses illustrating the surface wind field distribution for Hurricane Emily (left), Hurricane Katrina (center), and Hurricane Wilma (right) (courtesy of NOAA/AOML Hurricane Research Division).*

Another major observational advancement in the past decade is the development of the Scanning Radar Altimeter (SRA) (Walsh et al. 2002; Wright et al. 2001) that provides wave height and two-dimensional wave spectrum observations. The airborne wide-swath radar altimeter can also produce measurements of storm surge that provide validation metrics for assessing the accuracy of numerical storm surge models (Wright et al. 2009). The characteristic behavior of the swell relative to the local wind sea as a function of azimuth is shown in Fig. 2, from SRA measurements during Hurricane Ivan (2004) (from Black et al. 2007). The HRD H*Wind surface wind analysis (primarily derived from SFMR surface wind observations) is shown for Hurricane Ivan on 14 September 2004 when Ivan was translating to the northwest. Twelve SRA spectra located approximately 80 km from the eye are displayed. In the right-front quadrant, the wave field is characterized by a unimodal spectrum with ~350-m wavelength and an 11.4-m wave height maximum. Directly to the right of the track the

wavelength is considerably shorter (~260 m) and the spectrum becomes bimodal and broadens. To the right of track in the rear quadrant, the wave height is decreased and the spectrum is trimodal. The wave height and length reach minimum values of 5.6 m and 190 m in the rear quadrant; about half their values in the right-forward quadrant. Waves are young, steep, and short in the right-rear quadrant, in contrast to the older, flatter, and longer waves in the right-front and left-front quadrants. The wind and waves are nearly at right angles to each other to the left rear and left front quadrants. These wave characteristics are similar to other tropical cyclones, such as Bonnie, as described in Black et al. (2007).

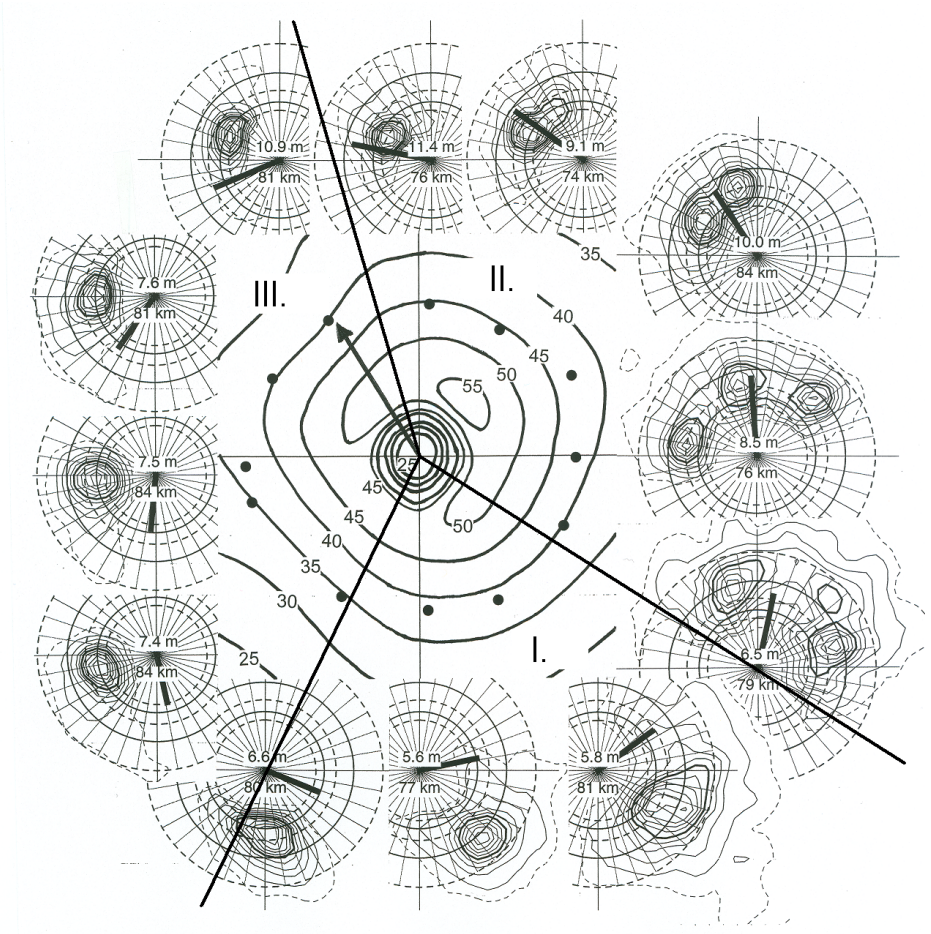

*Figure 2. The center of the figure shows wind speed contours (m s-1) from the HRD H*WIND surface wind analysis- based mainly on SFMR surface wind speed measurements in Hurricane Ivan at 2230 UTC on 14 September 2004 for a 2° box in latitude and longitude centered on the eye. Arrow at the center indicates Ivan's direction of motion (330°). The storm-relative locations of twelve 2D surface wave spectra measured by the SRA are indicated by the black dots. The spectra have nine solid contours linearly spaced between the 10% and 90% levels relative to the peak spectral density. The dashed contour is at the 5% level. The outer solid circle indicates a 200 m wavelength and the inner circle indicates a 300 m wavelength. The dashed circles indicate wavelengths of 150, 250, and 350 m (outer to inner). The thick line at the center of each spectrum points in the downwind direction, with its length proportional to the surface speed. The upper number at the center of each spectrum is the significant wave height and the lower number is the distance from the center of the eye. The average radial distance for the twelve spectral locations is 80 km. (from Black et al. 2007).*

3. Wind-Wave Interaction

The momentum exchange at the sea surface is dependent on the sea-state dependent drag coefficient, C_D. Prior to the past decade, the characteristics of C_D had never been observed in a tropical cyclone and was primarily based on extrapolations from field campaign measurements conducted in much weak wind conditions. In the hurricane-wind regime, the vertical variation of wind speed is controlled by the roughness of the sea surface (assuming neutral conditions). For neutral conditions, the mean wind speed (U) increases logarithmically with height (z), such that

$$U = (u_* / k) ln\left(z / z_0\right),$$

where the z_0 is the sea surface roughness length, u_* is the friction velocity, k is the von Kármán constant of 0.4. The surface momentum flux, τ, is defined as

$$\tau = \rho u_*^2 = \rho C_D U_{10}^2,$$

where ρ is the air density. The roughness length is typically described by the Charnock relationship

$$z_0 = \alpha u_*^2 / g,$$

where α is a constant most often defined between 0.01 and 0.035. In the general case, the Charnock "constant" depends on the characteristics of the surface wave spectrum. The most common property to characterize the dependence on the sea state is the wave age, C_p/u_*, where C_p is the wave phase speed at the spectral peak.

In a breakthrough study, Powell et al. (2003) used GPS dropwindsondes that had been deployed from aircraft and found a logarithmic variation of the mean wind speed in the lowest 200 m and a wind speed maximum at 500 m. They estimated the surface stress, roughness length, and neutral stability drag coefficient and found a markedly reduced drag coefficient at high wind speeds above 30 m s^{-1}. The analysis showed a leveling off of the surface momentum flux as the winds increase above the hurricane threshold and even a slight decrease of the drag coefficient with increasing wind speed.

Donelan et al. (2004) extended the Powell et al. (2003) study through a series of wind-wave tank experiments, as shown in Fig. 3. They found that a saturation of the drag coefficient occurs when the wind speed exceeds 33 m s^{-1}. Beyond this wind speed threshold, the surface roughness no longer increases. The saturation level for C_D that Donelan et al. found is 0.0025, similar to the saturation value of 0.0026 found by Powell et al. (2003). Shay and Jacob (2006) found that saturation occurs near 30 m s^{-1} with a drag coefficient of 0.0034. Jaroz et al. (2007) used current observations recorded during hurricane Ivan to estimate the momentum transfer from the ocean side of the air-sea interface. They found that for 20-48 m s^{-1} wind speeds, the drag coefficient initially increases and saturates at ~32 m s^{-1} before decreasing.

Bell et al. (2012) recognized that the exchange coefficients behavior is largely unknown at wind speeds greater than 50 m s^{-1}, which frequently occurs under hurricane conditions. They used absolute angular momentum and total energy budgets to derive the momentum and enthalpy fluxes based on an analysis of six missions conducted during the 2003 CBLAST field program in hurricanes Fabian

and Isabel. Their analysis, shown in Fig. 4, indicates a drag coefficient of 0.0024 for wind speeds between 52 and 72 m s^{-1}. The results are once again consistent with the notion that the drag levels off or even reduces as the wind speed increases beyond a threshold value of approximately 30 m s^{-1}.

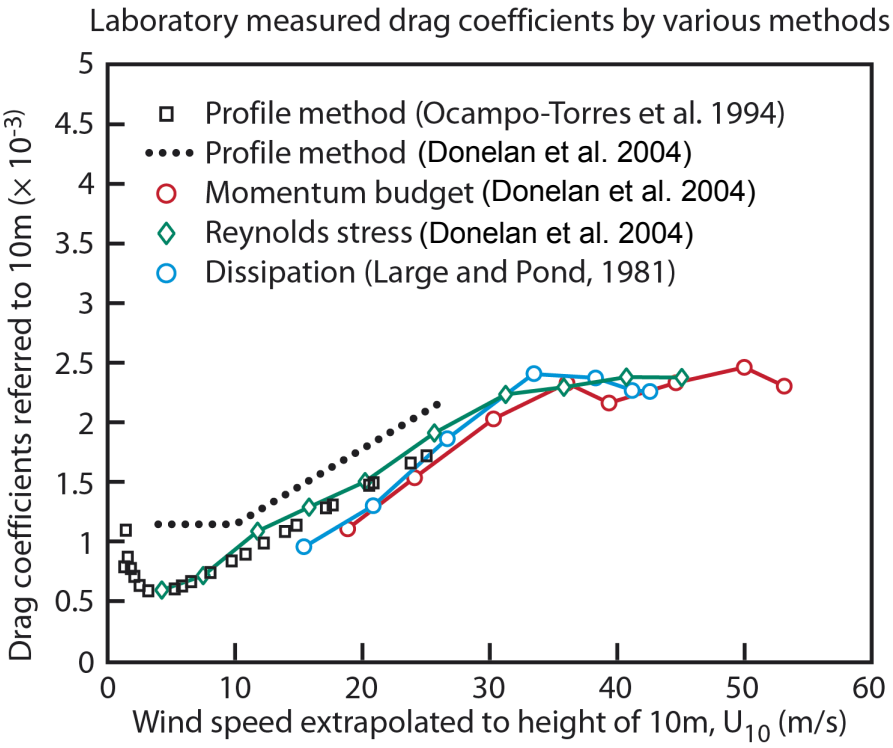

Figure 3. Laboratory measurements of the neutral stability drag coefficient (x 10^{-3}) by profile, Reynolds, and momentum budget methods. The drag coefficient refers to the wind speed measured at the standard anemometer height of 10 m. The drag coefficient relationship from Large and Pond (1981) is shown along with values from Ocampo-Torres et al. (1994) derived from field measurements. (Adapted from Donelan et al. 2004).

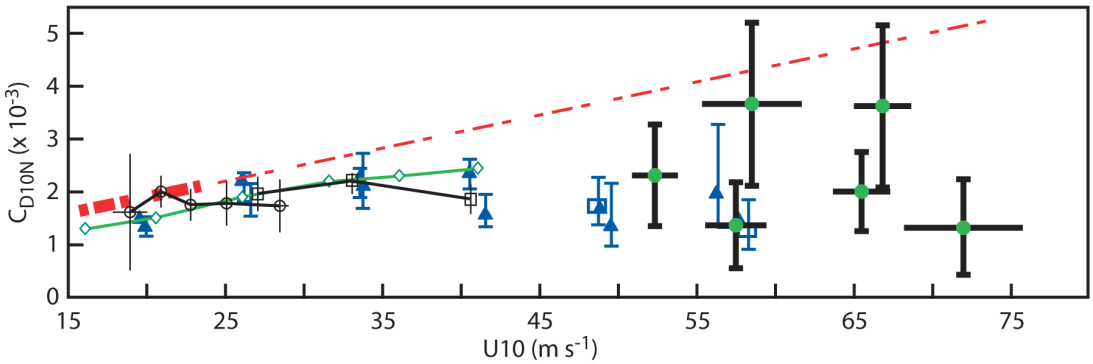

Figure 4. Wind speed dependence of C_D (Bell et al. 2012 study in green circles) compared with other studies of the drag coefficient in the high wind regime. Black symbols adapted from French et al. (2007) and blue symbols adapted from Vickery et al. (2009) are shown. The red line indicates measured (thick) and extrapolated (thin) Large and Pond (1981) drag coefficent. (From Bell et al. 2012)

During CBLAST, direct turbulent flux measurments were made in the hurricane boundary layer using a research aircraft, as summarized by Black et al. (2007). These measurments included estimates of the momentum and enthalpy flux exchange coefficients, which yielded unprecedented direct measurements of CK/CD in the hurricane-wind regime. These measurements extended the estimates of CK/CD into the high-wind regime by over 50% compared with previous studies. Zhang et al. (2008) derived the enthaply exchange coefficient based on CBLAST and found no evidence of an increase of C_K with wind speed. The mean ratio of C_K/C_D is 0.63, as shown in Fig. 5, which interestingly is below the threshold for hurricane development hypothesized by Emanuel (1995). Laboratory measurements conducted by Haus et al. (2010) provide air-sea heat and enthalpy transfer rates at even higher wind speeds than those measured during CBLAST. Their measurments suggest that the transfer coefficient ratio holds closely to a level of ~0.5 even in the highest observed winds. Bell et al. (2012) deduced momentum and enthalpy fluxes from absolute angular momentum and total energy budgets for Fabian and Isabel during CBLAST and found that the transfer coefficient ratio does not significantly increase with increasing wind speed, even for those greater than 50 m s^{-1}.

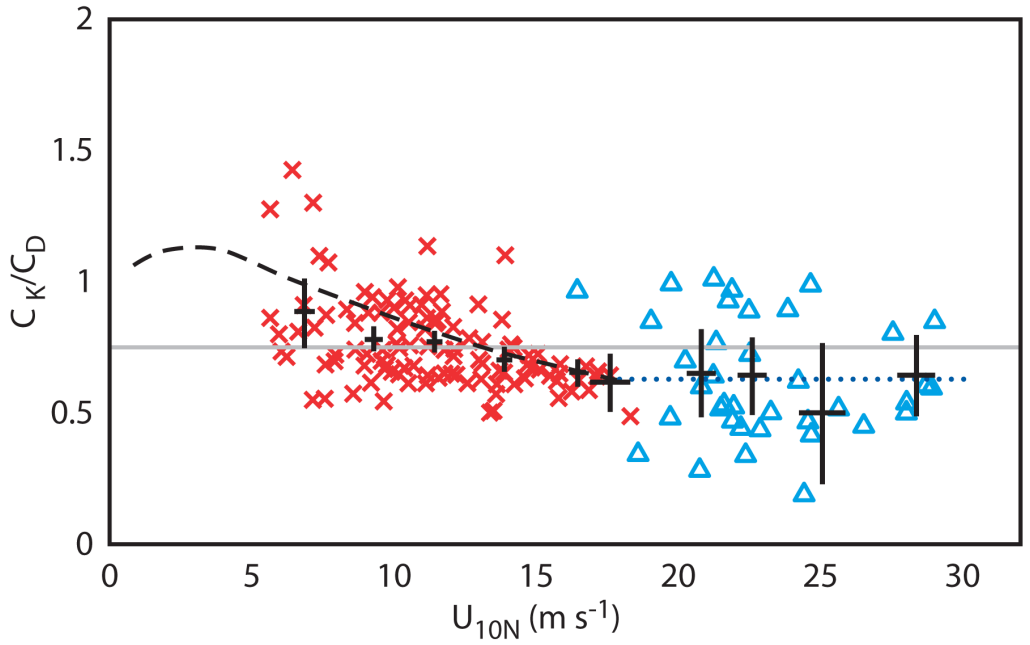

Figure 5. The ratio of C_K/C_D as a function of 10-m neutral wind speed. CBLAST (Δ), and Humidity Exchange Over the Sea (HEXOS) (x) measurements are shown. Solid black lines show the mean and 95% confidence intervals of the combined HEXOS and CBLAST field data. The dotted black line shows CBLAST mean. The ratio based on COARE 3.0 algorithm is shown as the dashed line. The ratio value of 0.75 as theorized by Emanuel is shown as the solid grey line (from Zhang 2008).

From a numerical modeling perspective, sea state, sea spray, and mixing within the upper portion of the ocean all contribute to important aspects of the air-sea interaction processes that occur beneath tropical cyclones and need to be properly represented. The conventional representation of the surface roughness effects over the sea due to ocean waves, based on the scaling arguments of Charnock (1955), is used by many atmospheric research and operational models, and is strictly valid only for

fully-developed ocean wave conditions. Under high-wind conditions, however, wind direction and speed are often time dependent, such as for a translating tropical cyclone. In these fetch-limited conditions, surface ocean waves have an increasingly important impact on the momentum flux in the atmospheric and oceanic boundary layers (Donelan 1990). In situations when the wave age is small, the wave-induced stress comprises a significant fraction of the total stress. A number of previous studies using field measurements have documented this dependence of the atmospheric momentum flux on the ocean wave age (e.g., Smith et al. 1992). The interaction between the sea and air is especially complex at high wind speeds where flux exchange processes may be impacted by sea spray (Kepert et al. 1999; Fairall et al. 2009). Wave-induced stress may be a significant component of the total momentum stress in the atmospheric boundary layer over the ocean (e.g., Donelan 1990; Janssen 1991) and has been suggested to enhance the decay of extratropical systems (e.g., Doyle 1995) and influence tropical cyclone structure and intensity (e.g., Bao et al. 2000; Doyle 2002; Chen et al. 2012).

The most established air-wave coupling methodology follows Janssen et al. (1989) and Janssen (1991) for the Wave Model (WAM) (WAMDI Group 1988) and includes the processes represented by mutual interaction of the wind waves and boundary-layer stress. The roughness length is represented by

$$z_o = \beta \frac{\tau}{g\rho(1-\tau_w/\tau)^{0.5}}, \quad (1)$$

where τ_w is the wave-induced stress. The constant β is chosen as 0.01 implying that (1) reduces to the standard Charnock relationship for a saturated wave state (τ_w=0). The wave-induced stress is defined as the integral over all directions and spectral components of the atmospheric momentum flux to the wind-generated wave field (Janssen 1989). For a young wind sea, it follows that the effective Charnock parameter can be enhanced by an order of magnitude. An iterative technique is used to calculate τ_w based on the wind speed, drag coefficient and stress. This coupling method using the WAM and an atmospheric model has been applied previously to study air-sea interaction in extratropical cyclones (e.g., Doyle 1995; Lionello et al. 1998; Desjardins et al. 2000; Lalbeharry et al. 2000) and tropical cyclones (Doyle 2002; Janssen 2008). The Janssen coupling technique using the WAM has been applied operationally at the European Center for Medium-Range Weather Forecasts (ECMWF) since 1998 and the results have indicated a substantial positive impact on the skill of the atmosphere and ocean wave model forecasts (Janssen et al. 2002). Desjardins et al. (2000) showed that an empirical sea state dependent z_0, based on data collected during the Humidity Exchange Over the Sea (HEXOS) experiment, yields consistent results with (1), which is of course strictly only valid for lower wind speeds.

Recently, several groups have applied fully coupled wind-wave models to tropical cyclones. Moon et al. (2004) developed a coupled wind-wave model capability that uses the surface wave directional frequency spectrum near the spectral peak based on the Wavewatch III (Tolman 2002) model, with the high frequency part of the spectrum parameterized following Hara and Belcher (2004). A wave boundary layer model is used along with the wave spectrum to estimate the Charnock coefficient. Their results show that the drag coefficient levels off at high-wind speeds and begins to decrease at ~35 m s^{-1} in agreement with field observations and laboratory measurements (Powell et al. 2003;

Donelan et al. 2004). Chen et al. (2012) describes a new approach to wind-wave coupling that includes a representation of the directionality of the wind and waves in hurricanes. The surface stress vector is calculated using the 2-dimensional wave spectra from a wave model that contains a modified spectral tail for the short waves. The wind and waves are coupled in a vector form in contrast to other methods that treat wave-induced roughness as a scalar. This new coupled parameterization was tested in a number of storms including Hurricane Frances (2004) during CBLAST. Without coupling to the surface waves, both the uncoupled atmospheric model and the coupled atmosphere-ocean model underestimate the surface wind speed. They found that the coupling with the directional wave-wind parameterization improves the model simulated surface wind flow including the wind inflow angle, which has an impact on the evolution and structure of Frances. The tropical cyclone version of the Coupled Ocean and Atmosphere Mesoscale Prediction System (COAMPS-TC^{TM}) (Doyle et al. 2012a) makes use of a community-based Earth System Modeling Framework to facilitate coupling to the Navy Coastal Ocean Model (NCOM) (Chen et al. 2010) and to the SWAN wave model (Smith et al. 2012). The two-way coupling between the ocean and wave models produces strong hurricane-induced currents that improve the overall simulated wave characteristics.

Recent research on sea spray has shown potentially important impacts on tropical cyclone intensity. Andreas et al. (2010) and Fairall et al. (2009) provide detailed parameterizations of sea spray effects in tropical cyclones. Sensitivity tests were conducted by Bao et al. (2011) using a new version of the Fairall spray parameterization that incorporates momentum and thermodynamic effects. The impact of sea-spray droplets on the mean profiles of wind, temperature, and moisture is shown to be a function of the winds at the spray generation level. As the wind speed increases, the mean droplet size and the mass flux of sea-spray increase, leading to a leveling-off of the surface drag due to an increase in the boundary layer stability. Sea spray also tends to increase the total air–sea sensible and latent heat fluxes at high winds.

4. Sensitivity to Fluxes

In this section, we illustrate the sensitivity of tropical cyclone intensity to surface fluxes. Many basic research questions related to tropical cyclones and air-sea interaction hinge on the notion of sensitivity. Addressing these sensitivity issues requires a method to quantify how particular aspects of the forecast will change based on peturbations to the model formulation or, as in this example, to changes in the initial or forecast state. To address the general question of sensitivity, one may employ an ensemble of NWP forecasts with perturbed initial conditions or model formulations. However, this approach often requires many model forecasts to fully span all of the possible forecast outcomes and may be computationally prohibitive. The adjoint, which technically is the transpose of the forward tangent propagator of the forecast model, allows one to find the sensitivity of a particular forecast output to changes in the initial state in a mathematically rigorous and computationally feasible manner (Errico 1997). In this section, we apply an adjoint of the Coupled Ocean/Atmosphere Mesoscale Prediction System (COAMPS®) atmospheric model (Amerault et al. 2008) to compute TC forecast sensitivity. The atmospheric model is coupled with a one-dimensional ocean mixed layer model.

Adjoint models provide the gradient of a scalar function J of the model state $\mathbf{x}_t$ at time t with respect to the initial state of the model $\mathbf{x}_{t0}$. Here, the three dimensional model state is expressed as a vector. This state vector depends on the initial and lateral boundary conditions of a nonlinear forecast model $\boldsymbol{M}$, and it follows that

$$J(x_t) = J[\boldsymbol{M}(x_{t0})]$$

For sensitivity applications, J is often referred to as the response function. The gradient of J with respect to the initial model state is given as

$$\frac{\partial J}{\partial x_{t0}} = \mathbf{M}^T \frac{\partial J}{\partial x_t}$$

where $\mathbf{M}$ is the tangent linear model of $\boldsymbol{M}$ and the superscript T denotes the transpose operation. The tangent linear model, which is the basis for the adjoint model, is created by linearizing the nonlinear model around the forecast trajectory of the nonlinear model. The adjoint model $\mathbf{M}^{\boldsymbol{T}}$ is formulated by realizing the transpose of the tangent linear model. Given that J is a continuous and differentiable function, the adjoint model forcing $\partial J/\partial \mathbf{x}_t$ is straightforward to compute by differentiating J with respect to the model state at time t.

The procedure to run an adjoint model for a sensitivity study begins with integration of the nonlinear forward model from the initial time t_0 to forecast time t, and the trajectory is saved at a predetermined frequency. The response function and adjoint forcing are computed at time t. Using the forcing as input and the nonlinear model trajectory to drive it, the adjoint model is run backwards to either t_0 or an earlier forecast time. This adjoint system has been successfully applied to study tropical cyclone initial condition sensitivity (Doyle et al. 2011; Doyle et al. 2012b).

We show an example of an adjoint sensitivity calculation in Fig. 6. The sensitivity of the low-level kinetic energy (proxy for storm intensity) in a box around the storm at the 18-h forecast time to the surface fluxes at 12-h for Typhoon Megi is shown in Fig. 6 during the rapid development stage at 1200-1800 UTC 16 October 2010. During this period, the simulated maximum 10-m wind speed increases by over 20% from 33 m s^{-1} to 40 m s^{-1}. The adjoint model uses a nested grid configuration with a horizontal grid increment of 27 km on the outer mesh and 9 km on the inner mesh. The model is nonhydrostatic and includes warm rain microphysics and a 1.5 order closure with a prognostic turbulence kinetic energy equation. A simple Kuo-type cumulus parameterization is used on the outer grid mesh. The momentum flux sensitivity (center panel in Fig. 6) shows that a reduction in the stress near the hurricane eye wall leads to an intensification, consistent with theoretical expectations. However, highly-structured banded regions of sensitivity are present in NE/SW quadrants. The sensitivity patterns indicate that an increase in the moisture flux (right panel) in the core leads to intensification, once again generally consistent with conventional understanding. Interestingly, isolated negative moisture flux sensitivity is located along the left flank of the storm. Overall, the sensitivity patterns underscore the complex nature of the interactions between the surface fluxes and the dynamics and thermodynamics of the storm.

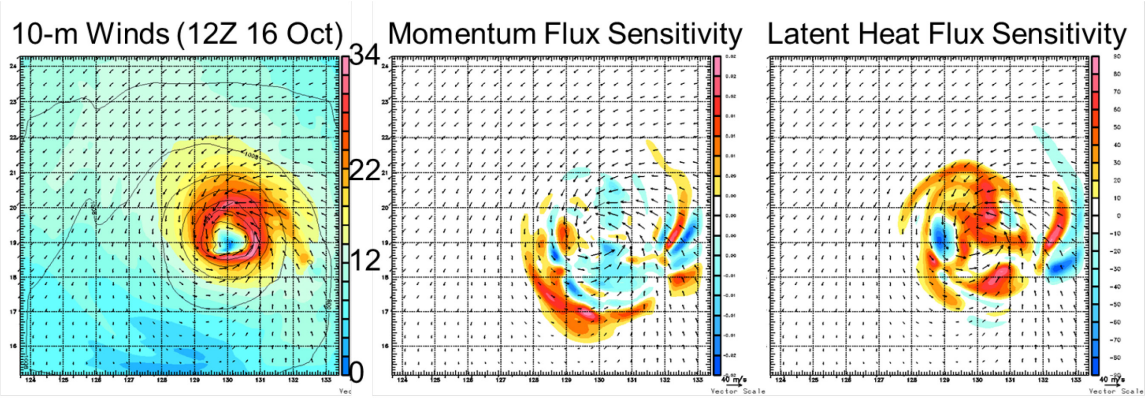

Figure 6 Adjoint sensitivity of the 18-h intensity (kinetic energy in the lowest 1 km surrounding the storm) of Typhoon Megi (2010) to the surface fluxes at the 12-h time. The 10-m winds (m s^{-1}) and sea-level pressure (hPa) at 12-h (1200 UTC 16 October 2010) (left), momentum flux sensitivity (m^2 s^{-2} (m^2 s^{-2})$^{-1}$, center) and latent heat flux sensitivity (m^2 s^{-2} (m s^{-1} kg kg^{-1})$^{-1}$, right) are shown, with the 10-m wind vectors for the second grid mesh (9 km resolution). The sensitivities are scaled by 10^5 km^{-3}.

5. Future Directions and Open Questions

In the past decade, there has been significant progress towards new insight and understanding of wind-wave interactions that occur beneath tropical cyclones. New observations, laboratory measurements, coupled models, and theoretical approaches have all contributed to these new advancements. One of the most significant advancements has been the discovery that the surface drag coefficient under hurricane conditions levels off or reaches a saturation value at approximately 30 m s^{-1}. Budget studies indicate that this saturation condition may hold up to 70 m s^{-1}. However, additional observations are needed in the high-wind regime to further extend the current drag coefficient results and establish the validity of budget study approaches. The ratio of the enthalpy coefficient and the drag coefficient appears to a key parameter governing tropical cyclones. It follows that the relationship between processes such as sea spray, surface fluxes, and TC intensity will remain an important avenue for research in the coming years.

Remaining questions regarding wind-wave interaction under hurricane conditions include:

- Does the drag coefficient remain nearly independent of wind speed beyond the current CBLAST-era observations of 30-35 m s^{-1}?
- What is the physical mechanism for reduced drag coefficients and saturation at high wind conditions?
- What new observational techniques and methods can best contribute to characterization of air-sea interaction processes in the high-wind regime?
- How does wave breaking and sea spray generation contribute to momentum and enthalpy fluxes, and how do these spray-modulated fluxes impact tropical cyclone intensity?

- What is the proper partitioning of stress into wave and current components, and how important is the partitioning under hurricane conditions?

- What is the significance of boundary layer rolls and log-law departures in the hurricane boundary layer for tropical cyclone structure and intensity?

- What is the most physically-realistic parameterization for wave-induced stress for coupled air-sea models in the high-wind regime?

- How important are sea-spray parameterizations for accurately forecasting hurricanes?

- What is the most consistent method of representing fluxes and budgets across the air-sea interface (and across processes) in high-resolution coupled models?

These questions should be addressed through analysis of new observational and laboratory measurements, coupled operational model results such as the ECMWF IFS, high-resolution coupled modeling studies of cases and events, and new theoretical investigations.

Acknowledgements

This research was supported by ONR PE0602435N and PE0601153N. Computing time was supported by a grant of HPC time from the DoD HPC DSRC at Stennis, MS. Isaac Ginnis and Shuyi Chen are acknowledged for helpful discussions for supplying some of the results summarized in this paper. Numerous illuminating discussions with Peter Janssen regarding ocean waves and air-sea interaction are greatly appreciated over the past years.

References

Amerault, C., X. Zou, and J Doyle, 2008: Tests of an Adjoint Mesoscale Model with Explicit Moist Physics on the Cloud Scale. *Mon. Wea. Rev*., **136**, 2120-2132.

Andreas, E.L, 2010: Spray-mediated enthalpy flux to the atmosphere and salt flux to the ocean in high winds. *J. Phys. Oceanogr*., **40**, 608-619.

Bao, J.-W., C. W. Fairall, S. A. Michelson, and L. Bianco, 2011: Parameterizations of sea-spray impact on the air-sea momentum and heat fluxes. *Mon. Wea. Rev*., **139**, 3781-3797.

Bao, J.-W., J.M. Wilczak, J.-K. Choi, and L.H. Kantha, 2000: Numerical simulations of air-sea interaction under high wind conditions using a coupled model: A study of hurricane development. *Mon. Wea. Rev*, **128**, 2190-2210.

Bell, M.M., M.T. Montgomery, and K.A. Emanuel, 2012: Air-sea enthalpy and momentum exchange at major hurricane wind speeds observed during CBLAST. *J. Atmos. Sci*. (to appear).

Black, P. G., E. A. D‟Asaro, W. Drennan, J. R. French, P. P. Niiler, T. B. Sanford, E. J. Terrill, E. J. Walsh, and J. Zhang, 2007: Air-sea exchange in hurricanes: synthesis of observations from the Coupled Boundary Layer Air-Sea Transfer experiment. *Bull. Amer. Meteor. Soc.,* **88**, 357-384.

Charnock, H., 1955: Wind stress on a water surface. Quart. J. Roy. Meteor. Soc., 81, 639-640.

Chen, S., Campbell, T.J., Jin, H., Gaberšek, S., Hodur, R.M., Martin, P.J., 2010. Effect of two-way air-sea coupling in high and low wind speed regimes. *Mon. Wea. Rev*. **138**, 3579–3602.

Chen, S.S., W. Zhao, M.A. Donelan, H. Tolman, 2012: Directional wind-wave coupling in fully coupled atmosphere-wave-ocean models: Results from CBLAST-Hurricane. Submitted to *J. Atmos. Sci*.

Desjardins, S. J. Mailhot, R. Lalbeharry, 2000: Examination of the impact of a coupled atmospheric and ocean wave system. Part I. Atmospheric aspects. *J. Phys. Oceanogr*., **30**, 385-401.

Donelan, M. A., B. K. Haus, N. Reul, W. J. Plant, M. Stiassine, H. Graber, O. Brown, and E. Saltzman, 2004: On the limiting aerodynamic roughness of the ocean in very strong winds. *Geophys. Res. Letters*., 31L18306,doi:1029/2004GRL019460.

Donnelan, M., 1990: Air sea interaction. *Surface Waves and Fluxes, Vol. 1*. Edited by G.L. Geernaert and W.J. Plant, 336 pp., Kluwer Acad., Norwell Mass.

Doyle, J. D., 1995: Coupled ocean wave/atmosphere mesoscale model simulations of cyclogenesis. *Tellus*, **47A**, 766-788.

Doyle, J.D., 2002: Coupled atmosphere-ocean wave simulations under high wind conditions. *Mon. Wea. Rev*., **130**, 3087-3099.

Doyle, J.D., C.A. Reynolds, C. Amerault, 2011: Diagnosing tropical cyclone sensitivity. *Computing in Science and Engineering*, **13**, 31-39.

Doyle J., Jin, Y., Hodur, R.M., Chen, S., Jin, H., Moskaitis, J., Reinecke, A., Black, P., Cummings, J., Hendricks, E., Holt, T., Liou, C.-S., Peng, M., Reynolds, C., Sashegyi, K., Schmidt, J., Wang S., 2012a. Real-time tropical cyclone prediction using COAMPS-TC. *Advances in Geosciences*. In press.

Doyle, J.D., C.A. Reynolds, C. Amerault, J. Moskaitis, 2012b: Adjoint sensitivity and predictability of tropical cyclogenesis. Submitted to *J. Atmos. Sci.*

Emanuel, K A., 1986: An air-sea interaction theory for tropical cyclones Part 1: Steady-State maintenance**.** *J. Atmos. Sci.***, 43,** 585-605.

Emanuel, K A., 1995: Sensitivity of tropical cyclones to surface exchange and a revised steady-state model incorporating eye dynamics**.** *J. Atmos. Sci.***, 52,** 3969-3976.

Fairall, C.W., M. Banner, W. Peirson, R. P. Morison, and W. Asher, 2009: Investigation of the physical scaling of sea spray spume droplet production. *J. Geophys., Res*., **114**, C10001, doi:10.1029/2008JC004918.

French, J. R., W. M. Drennan, J. A. Zhang, and P. G. Black, 2007: Turbulent fluxes in the hurricane boundary layer. Part 1: Momentum flux. *J. Atmos. Sci.*, **64,** 1089-1102.

Hara, T., and S. E. Belcher, 2004: Wind profile and drag coefficient over mature ocean surface wave spectra. *J. Phys. Oceanogr*., **34,** 2345-2358.

Haus, B. K., D. Jeong, M. A. Donelan, J. A. Zhang, and I. Savelyev (2010), Relative rates of sea-air heat transfer and frictional drag in very high winds, *Geophys. Res. Lett*., **37**, L07802, doi:10.1029/2009GL042206.

Janssen, P.A.E.M, 2008: Air-sea interaction through wave. *ECMWF Workshop on Ocean-Atmosphere Interactions*, 10-12 November 2008, 47-60.

Janssen, P.A.E.M., 1989: Wave-induced stress and the drag of air flow over sea waves. *J. Phys. Oceanogr.*, **19**, 745-754.

Janssen, P.A.E.M., 1991: Quasi-linear theory of wind-wave generation applied to wave forecasting. *J. Phys. Oceanogr.*, **21**, 1631-1642.

Janssen, P.A.E.M., J. D. Doyle, J. Bidlot, B. Hansen, L. Isaksen and P. Viterbo, 2002. Impact and feedback of ocean waves on the atmosphere. Pp. 155-197 in *Advances in fluid mechanics. Atmosphere-ocean interactions. Vol. 1,* Ed. W. Perrie*,* WITpress

Jarosz, E., D.A. Mitchell, D.W. Wang, and W.J. Teague, 2007: Bottom-up determination of air-sea momentum exchange under a major tropical cyclone. *Science*, **315**, 1707.

Kepert, J.D, C.W. Fairall and J.W. Bao, 1999: Modelling the interaction between the atmospheric boundary layer and evaporating sea spray droplets. *Air-Sea Fluxes of Momentum, Heat and Chemicals*. editor G.L Geeraert. Kluwer.

Lalbeharry, R., J. Mailhot, S. Desjardins, and L. Wilson, 2000: Examination of the impact of a coupled atmospheric and ocean wave system. Part II: Ocean wave aspects. *J. Phys. Oceanogr.*, **30**, 402-415.

Large, W.G., and S. Pond, 1981: Open ocean momentum flux measurements in moderate to strong winds. J. *Phys. Oceanogr.*, **11,** 324-336, 1981.

Lionello, P., P. Malguzzi and A. Buzzi, 1998: Coupling between the atmospheric circulation and ocean wave field: An idealized case. *J. Phys. Oceanogr.*, **28**, 161-177.

Moon, I., I. Ginis, and T. Hara, 2004: Effect of surface waves on Charnock coefficient under tropical cyclones. *Geophys. Res. Lett.*, **31**, L20302.

Ocampo-Torres, F.J., M.A. Donelan, N. Merzi, and F. Jia, 1994: Laboratory measurements of mass transfer of carbon dioxide and water vapour for smooth and rough flow conditions. *Tellus*, **46B**, 16-32.

Ooyama K., 1969: Numerical simulation of the life cycle of tropical cyclones. *J. Atmos. Sci.*, **26**, 3–40.

Powell, M. D., S. Murillo, P. Dodge, E. Uhlhorn, J. Gamache, V. Cardone, A. Cox, S. Otero, N. Carrasco, B. Annane, and R. St. Fleur, 2010: Reconstruction of Hurricane Katrina's wind fields for storm surge and wave hindcasting. Ocean Engineering, 37, 26-36.

Powell, M.D., P.J. Vickery, and T.A. Reinhold, 2003: Reduced drag coefficient for high wind speeds in tropical cyclones. *Natur*e, **422,** 279-283.

R.M. Errico, 1997: What is an adjoint model. *Bull. Amer. Meteor. Soc*., **78**, 2577-2591.

Shay, L. K, and S. D. Jacob, 2006: Relationship between oceanic energy fluxes and surface winds during tropical cyclone passage (Chapter 5). Atmosphere-Ocean Interactions II, *Advances in Fluid Mechanics*. Ed. W. Perrie, WIT Press, Southampton, UK, 115-142.

Shay, L.K., 2011: Air-sea interface and oceanic influences. *Seventh International Workshop on Tropical Cyclones.* WMO/CAC/WWW, La Réunion Island. 48 pp.

Smith, S.D., R.J. Anderson, W.A. Oost, C. Kraan, N. Maat, J. De Cosmo, K.B. Katsaros, K. Davidson, K. Bumke, L. Hasse, and H.M. Chadwick, 1992: Sea surface wind stress and drag coefficients. The HEXOS results. *Bound Layer Meteor*., **60**, 109-142.

Smith, T.A., S. Chen, T. Campbell, E. Rogers, S. Gabersek, D. Wang, S. Carroll, R. Allard, 2012: Ocean-wave coupled modeling in COAMPS-TC: A study of hurricane Ivan (2004). Submitted to *Ocean Modelling*.

The WAMDI Group (S. Hasselmann et al.), 1988: The WAM model - a third generation ocean wave prediction model. *J. Phys. Oceanogr*., **18**, 1775-1810.

Tolman, H. L., 2002: User manual and system documentation of WAVEWATCH-III version 2.22. NOAA/NWS/NCEP/OMB Tech. Note 222, 133 pp.

Uhlhorn, E. W., P. G. Black, J. L. Franklin, M. Goodberlet, J. Carswell and A. S. Goldstein, 2007:Hurricane surface wind measurements from an operational stepped frequency microwave radiometer. *Mon. Wea. Rev*., **135,** 3070-3085.

Vickery, P. J., D. Wadhera, M. D. Powell, and Y. Chen, 2009: A hurricane boundary layer and wind field model for use in engineering applications. *J. Appl. Meteor. Climat*., **48**, 381-405.

Walsh, E.J., and Coauthors, 2002: Hurricane directional wave spectrum spatial variation at landfall. *J. Phys. Oceanogr*., **32**, 1667–1684.

Wright, C. W., and Coauthors, 2009: Measuring Storm Surge with an Airborne Wide-Swath Radar Altimeter. *J. Atmos. Oceanic Technol.*, **26**, 2200–2215.

Wright, C. W., E. J. Walsh, D. Vandemark, W. B. Krabill, A. W. Garcia, S. Houston, M. Powell, P. Black, and F. D. Marks, 2001: Hurricane directional wave spectrum spatial variations in the open ocean. *J. Phys. Oceanogr.,* **31**, 2472-2488.

Wright, C. W., E. J. Walsh, D. Vandemark, W. B. Krabill, A. W. Garcia, S. Houston, M. Powell, P. Black, and F. D. Marks, 2001: Hurricane directional wave spectrum spatial variations in the open ocean. *J. Phys. Oceanogr.,* **31**, 2472-2488.

Zhang, J. A., P. G. Black, J. R. French, and W. M. Drennan, 2008: First direct measurements of enthalpy flux in the hurricane boundary layer: The CBLAST results. *Geophys. Res. Lett*., **35**, L14 813. doi:10.1029/2008GL034 374.